J|A|C|S
ARTICLES
Published on Web 09/29/2007

Small Molecule Inhibitors of the MDM2-p53 Interaction Discovered by Ensemble-Based Receptor Models

Anna L. Bowman,[†] Zaneta Nikolovska-Coleska,[‡,§] Haizhen Zhong,[†,||] Shaomeng Wang,[†,‡,§] and Heather A. Carlson*[,†]

Contribution from the Departments of Medicinal Chemistry and Internal Medicine and the Comprehensive Cancer Center, University of Michigan, Ann Arbor, Michigan 48109

Received May 22, 2007; E-mail: carlsonh@umich.edu

Abstract: Five nonpeptide, small-molecule inhibitors of the human MDM2−p53 interaction are presented, and each inhibitor represents a new scaffold. The most potent compound exhibited a K_i of 110 ± 30 nM. These compounds were identified using our multiple protein structure (MPS) method which incorporates protein flexibility into a receptor-based pharmacophore model that identifies appropriate hotspots of binding. Docking the inhibitors with an induced-fit docking protocol suggested that the inhibitors mimicked the three critical binding residues of p53 (Phe19, Trp23, and Leu26). Docking also predicted a new orientation of the scaffolds that more fully fills the binding cleft, enabling the inhibitors to take advantage of additional hydrogen-bonding possibilities not explored by other small molecule inhibitors. One inhibitor in particular was proposed to probe the hydrophobic core of the protein by taking advantage of the flexibility of the binding cleft floor. These results show that the MPS technique is a promising advance for structure-based drug discovery and that the method can truly explore broad chemical space efficiently in the quest to discover potent, small-molecule inhibitors of protein−protein interactions. Our MPS technique is one of very few ensemble-based techniques to be proven through experimental verification of the discovery of new inhibitors.

Introduction

The p53 tumor suppressor is vital in cell cycle regulation, DNA repair, and apoptosis.[1−3] Mutations in p53 are seen in approximately 50% of all human cancers.[4] In the remaining 50%, p53 is in wild-type form, yet is inhibited by overexpression[5,6] or amplification[7] of murine double minute 2 oncoprotein (MDM2; also frequently referred to as HDM2 in human). Hence, these cancers are tolerant to elevated levels of wild-type p53. Reactivation of p53 through inhibition of the p53−MDM2 interaction has been shown to be a novel approach for initiating or enhancing cancer cell death.[8,9]

Oligomers that mimic the bound p53 helix have been shown to disrupt the p53−MDM2 interaction.[10−14] However, inhibition with small molecules is a more attractive proposal due to the pharmacological advantages of small molecule drugs such as enhanced stability and oral bioavailability.[15] Because of their large and shallow interfaces, protein−protein interactions are notoriously difficult to inhibit with small molecules.[16] However, MDM2−p53 presents a deep well-defined binding cleft favorable to inhibition with small molecules.[17−19]

X-ray crystallography has shown that three critical binding residues in p53 (Phe19, Trp23, and Leu26) on a short α-helix interact with the binding cleft of MDM2.[17] The importance of these residues has been confirmed both experimentally[19] and computationally.[18] Varied approaches have been employed to identify nonpeptide, small-molecule inhibitors targeting the MDM2−p53 interaction by mimicking these key residues.[15,20] Identification of lead molecules with experimental high-throughput screening has led to potent antagonists of the MDM2−p53 interaction such as the nutlins,[21] 1,4-benzodiazepine-

[†] Department of Medicinal Chemistry.
[‡] Department of Internal Medicine.
[§] Comprehensive Cancer Center.
[||] Present address: University of North Carolina−Greensboro.

(1) Vogelstein, B.; Lane, D.; Levine, A. J. *Nature* **2000**, *408*, 307−310.
(2) Levine, A. J. *Cell* **1997**, *88*, 323−331.
(3) Lane, D. P. *Nature* **1992**, *358*, 15−16.
(4) Soussi, T.; Dehouche, K.; Beroud, C. *Hum. Mutat.* **2000**, *15*, 105−113.
(5) Eymin, B.; Gazzeri, S.; Brambilla, C.; Brambilla, E. *Oncogene* **2002**, *21*, 2750−2761.
(6) Polsky, D.; Bastian, B. C.; Hazan, C.; Melzer, K.; Pack, J.; Houghton, A.; Busam, K.; Cordon-Cardo, C.; Osman, I. *Cancer Res.* **2001**, *61*, 7642−7646.
(7) Momand, J.; Jung, D.; Wilczynski, S.; Niland, J. *Nucleic Acids Res.* **1998**, *26*, 3453−3459.
(8) Chène, P. *Nat. Rev. Cancer* **2003**, *3*, 102−109.
(9) Vassilev, L. T. *J. Med. Chem.* **2005**, *48*, 4491−4499.
(10) Hara, T.; Durell, S. R.; Myers, M. C.; Appella, D. H. *J. Am. Chem. Soc.* **2006**, *128*, 1995−2004.
(11) Garcia-Echeverria, C.; Chène, P.; Blommers, M. J. J.; Furet, P. *J. Med. Chem.* **2000**, *43*, 3205−3208.
(12) Fasan, R.; Dias, R. L. A.; Moehle, K.; Zerbe, O.; Obrecht, D.; Mittl, P. R. E.; Grutter, M. G.; Robinson, J. A. *ChemBioChem* **2006**, *7*, 515−526.
(13) Kritzer, J. A.; Lear, J. D.; Hodsdon, M. E.; Schepartz, A. *J. Am. Chem. Soc.* **2004**, *126*, 9468−9469.
(14) Oliner, J. D.; Pietenpol, J. A.; Thiagalingam, S.; Gvuris, J.; Kinzler, K. W.; Vogelstein, B. *Nature* **1993**, *362*, 857−860.
(15) Buolamwini, J. K.; Addo, J.; Kamath, S.; Patil, S.; Mason, M.; Ores, M. *Curr. Cancer Drug Targets* **2005**, *5*, 57−68.
(16) Whitty, A.; Kumaravel, G. *Nat. Chem. Biol.* **2006**, *2*, 112−118.
(17) Kussie, P. H.; Gorina, S.; Marechal, V.; Elenbaas, B.; Moreau, J.; Levine, A. J.; Pavletich, N. P. *Science* **1996**, *274*, 948−953.
(18) Massova, I.; Kollman, P. A. *J. Am. Chem. Soc.* **1999**, *121*, 8133−8143.
(19) Böttger, A.; Böttger, V.; Garcia-Echeverria, C.; Chène, P.; Hochkeppel, H.-K.; Sampson, W.; Ang, K.; Howard, S. F.; Picksley, S. M.; Lane, D. P. *J. Mol. Biol.* **1997**, *269*, 744−756.
(20) Fischer, P. M. *Int. J. Pept. Res. Ther.* **2006**, *12*, 3−19.

2,5-diones,[22−26] and isoindolinone-based compounds.[27,28] The recently reported spiro-oxindoles were developed by a *de novo* computational structure-based approach.[29,30] Other inhibitors were proposed through the design of a scaffold to preorient side chains to mimic the three key residues of p53.[31,32] Galatin and Abraham presented a nontraditional pharmacophore model, based on the X-ray crystal structure of p53 bound to MDM2,[17] where explicit atoms including distance and angle restraints were entered into a 3D database searching program.[33] The model was used to screen the NCI chemical database with a distance tolerance of ±20%; this resulted in the identification of a sulfonamide compound which was found to be a low-affinity inhibitor of the MDM2−p53 interaction with an IC_{50} of 31.8 μM.[34] A simple pharmacophore model, consisting of only the three hydrophobic elements, was recently proposed based on the p53 peptide and known small molecule inhibitors of MDM2. The resultant compounds from a screen of the NCI database with this pharmacophore model were then docked and ranked, which led to the identification of the potent inhibitor NSC 66811 with a K_i of 120 nM.[35]

Here, we progress from the simple ligand-based pharmacophore models previously reported to propose a dynamic, receptor-based pharmacophore model of MDM2. We employ our method which incorporates protein flexibility by utilizing multiple protein structures (MPS) to represent an ensemble of conformational states. We map out complementary interactions with the binding site using probe molecules. The probes identify conserved regions of the protein where the same interactions are consistently made with the majority of the MPS despite the inherent motion of the active site.[36,37] This is equivalent to identifying binding hotspots that are conserved over the protein dynamics. The models are used to search databases and identify compounds which have features that fulfill the conserved binding pattern. No limits are placed in flexible regions, allowing us to identify compounds with different sizes, shapes, and scaffolds. The conformational states of the protein can be taken from a molecular dynamic simulation,[37−39] X-ray crystallographic structures,[36,40] or an NMR ensemble.[41] The method, initially applied to HIV integrase,[37] has been successfully extended to HIV-1 protease[38,39,41] and dihydrofolate reductase.[40]

In this study, we present the results of a high-throughput virtual screening of a modest database. Our model of the cleft of MDM2, which encodes chemical and dynamics features of the site, has identified five novel scaffolds which inhibit the MDM2−p53 interaction. This builds upon the proven ability of the MPS method in distinguishing known inhibitors over druglike noninhibitors.[38−41] The results demonstrate the power of the MPS method in expanding relevant chemical space and identifying diverse, new inhibitors.

Methods

Computational Protein Preparation. NMR studies of apo MDM2 revealed that the more open conformation afforded by bound MDM2 is more suitable to computer-aided drug discovery,[42] and so we focused on bound structures of the target. Snapshots were taken every 100 ps from a 2-ns molecular dynamics simulation of human MDM2 bound to p53.[32] This resulted in 21 structures for MDM2. The variation was analyzed through rmsd measurements across the set (210 unique comparisons; see Supporting Information). The structures show good diversity and well represent the local conformational variation of this p53-bound state.

Probe Flooding, Minimization, and Clustering. All solvent molecules and the p53 peptide were removed from each structure. The binding cleft of each structure was flooded with 1000 small-molecule probes using a 15 Å sphere centered on Phe86 Hζ. The probes used for flooding were benzene to identify aromatic and hydrophobic interactions, ethane to distinguish hydrophobic interactions from aromatic, and methanol to identify hydrogen-bonding interactions. The probes were then optimized through a low-temperature Monte Carlo minimization, in BOSS,[43] using the OPLS force field.[44] The probes undergo simultaneous multiple gas-phase minimizations, while the protein is held fixed, to reveal complementary binding regions.[37] The probes were then grouped into clusters using an in-house Jarvis−Patrick automated clustering procedure, and only clusters of eight or more probes were considered significant local minima on the surface. Each cluster was then represented by the lowest-energy probe in the group, termed its "parent".

The snapshots were overlaid to the equilibration structure using a Gaussian-weighted rmsd alignment.[45] The parent probes from each structure within 12 Å of Ile61 Cδ1 were combined and clustered to give "consensus clusters". A consensus cluster must contain parents from ≥50% of the protein conformations. Each consensus cluster was represented as a spherical pharmacophore element. The center of each element was defined by the average position of the parent probes in the consensus cluster, and the radius was given by the rmsd of those probes.[38] The MPS routine creates pharmacophore models which focus on elements conserved across multiple conformations; flexibility is implicitly accommodated by not limiting the chemical requirements in flexible regions of the pocket. As long as the rather stringent requirements of the consensus region are met, an identified compound

(21) Vassilev, L. T.; Vu, B. T.; Graves, B.; Carvajal, D.; Podlaski, F.; Filipovic, Z.; Kong, N.; Kammlott, U.; Lukacs, C.; Klein, C.; Fotouhi, N.; Liu, E. A. *Science* **2004**, *303*, 844−848.
(22) Parks, D. J., et al. *Bioorg. Med. Chem. Lett.* **2006**, *16*, 3310−3314.
(23) Parks, D. J.; LaFrance, L. V.; Calvo, P. R.; Milkiewicz, K. L.; Gupta, V.; Lattanze, J.; Ramachandren, K.; Carver, T. E.; Petrella, E. C.; Cummings, M. D.; Maguire, D.; Grasberger, B. L.; Lu, T. *Bioorg. Med. Chem. Lett.* **2005**, *15*, 765−770.
(24) Raboisson, P.; Marugan, J. J.; Schubert, C.; Koblish, H. K.; Lu, T. B.; Zhao, S. Y.; Player, M. R.; Maroney, A. C.; Reed, R. L.; Huebert, N. D.; Lattanze, J.; Parks, D. J.; Cummings, M. D. *Bioorg. Med. Chem. Lett.* **2005**, *15*, 1857−1861.
(25) Grasberger, B. L., et al. *J. Med. Chem.* **2005**, *48*, 909−912.
(26) Koblish, H. K., et al. *Mol. Cancer Ther.* **2006**, *5*, 160−169.
(27) Hardcastle, I. R., et al. *Bioorg. Med. Chem. Lett.* **2005**, *15*, 1515−1520.
(28) Hardcastle, I. R., et al. *J. Med. Chem.* **2006**, *49*, 6209−6221.
(29) Ding, K.; Lu, Y.; Nikolovska-Coleska, Z.; Qiu, S.; Ding, Y.; Gao, W.; Stuckey, J.; Krajewski, K.; Roller, P. P.; Tomita, Y.; Parrish, D. A.; Deschamps, J. R.; Wang, S. *J. Am. Chem. Soc.* **2005**, *127*, 10130−10131.
(30) Ding, K.; Lu, Y. P.; Nikolovska-Coleska, Z.; Wang, G. P.; Qiu, S.; Shangary, S.; Gao, W.; Qin, D. G.; Stuckey, J.; Krajewski, K.; Roller, P. P.; Wang, S. M. *J. Med. Chem.* **2006**, *49*, 3432−3435.
(31) Lu, F.; Chi, S. W.; Kim, D. H.; Han, K. H.; Kuntz, I. D.; Guy, R. K. *J. Comb. Chem.* **2006**, *8*, 315−325.
(32) Zhong, H.; Carlson, H. A. *Proteins* **2005**, *58*, 222−234.
(33) Galatin, P. S.; Abraham, D. J. *Proteins* **2001**, *45*, 169−175.
(34) Galatin, P. S.; Abraham, D. J. *J. Med. Chem.* **2004**, *47*, 4163−4165.
(35) Lu, Y. P.; Nikolovska-Coleska, Z.; Fang, X. L.; Gao, W.; Shangary, S.; Qiu, S.; Qin, D. G.; Wang, S. M. *J. Med. Chem.* **2006**, *49*, 3759−3762.
(36) Carlson, H. A.; Masukawa, K. M.; McCammon, J. A. *J. Phys. Chem. A* **1999**, *103*, 10213−10219.
(37) Carlson, H. A.; Masukawa, K. M.; Rubins, K.; Bushman, F. D.; Jorgensen, W. L.; Lins, R. D.; Briggs, J. M.; McCammon, J. A. *J. Med. Chem.* **2000**, *43*, 2100−2114.
(38) Meagher, K. L.; Carlson, H. A. *J. Am. Chem. Soc.* **2004**, *126*, 13276−13281.
(39) Meagher, K. L.; Lerner, M. G.; Carlson, H. A. *J. Med. Chem.* **2006**, *49*, 3478−3484.
(40) Bowman, A. L.; Lerner, M. G.; Carlson, H. A. *J. Am. Chem. Soc.* **2007**, *129*, 3634−3640.
(41) Damm, K. L.; Carlson, H. A. *J. Am. Chem. Soc.* **2007**, *129*, 8225−8235.
(42) Uhrinova, S.; Uhrin, D.; Powers, H.; Watt, K.; Zheleva, D.; Fischer, P.; McInnes, C.; Barlow, P. N. *J. Mol. Biol.* **2005**, *350*, 587−598.
(43) Jorgensen, W. L. *BOSS*, version 4.2; Yale University: New Haven, CT, 2000.
(44) Jorgensen, W. L.; Maxwell, D. S.; Tirado-Rives, J. *J. Am. Chem. Soc.* **1996**, *118*, 11225−11236.
(45) Damm, K. L.; Carlson, H. A. *Biophys. J.* **2006**, *90*, 4558−4573.

can have any other chemical features. To loosely include steric constraint of the pocket, seven excluded volume elements were added to complete the pharmacophore model. These had a radius of 1.5 Å and were centered at the average position of Met50 Cβ, Leu54 Cβ, Leu57 Cβ, Gly58 Cα, Gln72 Cα, Val93 Cβ, and Tyr100 Cβ.

Model Generation and Virtual Screening. The model required all pharmacophore elements to be satisfied and the radius of each pharmacophore element, given by the rmsd of the consensus cluster, to be increased by a multiplication factor of 2. Additionally, a model in which we attempt to take advantage of a possible different binding mode was created. A hydrophobic pocket which was previously reported by our group[32] was also incorporated by adding a hydrophobic element of radius 1.0 Å and reducing the stringency of other requirements (see Results). The University of Michigan's Center for Chemical Genomics' database of ~35 000 commercially available compounds was used for screening. The compounds were "washed" in MOE.[46] "Washing" removed water molecules, counterions, simple acids and bases, common solvents, and salts to leave just a single component. Ionization states were set to their formal charge. Acids were deprotonated, and bases, protonated. Multiple conformations of each compound were generated using rule-based torsion driving in OMEGA[47] using an energy cutoff of 14 kcal/mol and a heavy-atom rmsd criterion of 1 Å. The MDM2 pharmacophore models were screened against the database using MOE.[46] This resulted in several attractive hits which went on for experimental testing.

Fluorescence Polarization Competitive MDM2 Binding Assay. The compounds identified as possible MDM2 inhibitors were purchased from ChemDiv and Chembridge. For testing their binding affinities to the MDM2 protein, we have optimized and established a sensitive and quantitative FP-based binding assay using human recombinant His-fused soluble protein MDM2 (residues 1−118) and a p53-based peptide labeled with a fluorescence tag, termed as **PMDM6-F**. The design of a fluorescence probe was based upon a previously reported high-affinity peptide-based inhibitor (5-FAM-βAla-βAla-Phe-Met-Aib-pTyr-(6-Cl-L-Trp)-Glu-Ac3c-Leu-Asn-NH2) of the MDM2−p53 interaction.[11] The K_d value of **PMDM6-F** with the MDM2 protein was determined to be 2.22 nM ± 0.09, consistent with its reported high affinity. The specificity of the assay was confirmed by competitive displacement of **PMDM6-F** from the MDM2 protein by its corresponding unlabeled peptide (termed PMDM6) without the fluorescence tag 5-FAM. As an additional control, we have synthesized and tested the natural p53 peptide (PLSQETFSDLWKLLPEN-NH2), which has a K_i value of 6.67 ± 1.24 μM in our binding assay, similar to the values reported in literature.

The dose-dependent binding experiments were carried out with serial dilutions of the tested compounds in DMSO. A 5 μL sample of the tested samples and preincubated MDM2 protein (10 nM) and **PMDM6-F** peptide (1 nM) in the assay buffer (100 mM potassium phosphate, pH 7.5; 100 μg/mL bovine gamma globulin; 0.02% sodium azide, purchased from Invitrogen Life Technology) were added in Dynex 96-well, black, round-bottom plates (Fisher Scientific) to produce a final volume of 125 μL. For each assay, the controls included the MDM2 protein and **PMDM6-F** (equivalent to 0% inhibition) and only the **PMDM6-F** peptide (equivalent to 100% inhibition). The polarization values were measured after 3 h of incubation using an ULTRA READER (Tecan U.S. Inc., Research Triangle Park, NC). The IC_{50} values, i.e., the inhibitor concentration at which 50% of bound peptide is displaced, were determined from a plot using nonlinear least-squares analysis. Curve fitting was performed using GRAPHPAD PRISM software (GraphPad Software, Inc., San Diego, CA). To calculate the binding affinity constants (K_i) of inhibitors, we have used the following equation developed for computing the K_i values in FP-based binding assays:

$$K_i = [I]_{50}/([L]_{50}/K_d + [P]_0/K_d + 1)$$

in which $[I]_{50}$ denotes the concentration of the free inhibitor at 50% inhibition, $[L]_{50}$, the concentration of the free labeled ligand at 50% inhibition, $[P]_0$, the concentration of the free protein at 0% inhibition, and K_d, the dissociation constant of the protein−ligand complex. We developed a computational procedure to compute accurate values of all of the parameters used in the equation. A web-based computer program was developed for computing the K_i values for inhibitors in FP-based binding assays based upon this equation.[48]

Induced-Fit Docking. Recently, an IFD procedure has been reported which combines rigid-receptor docking with protein refinement.[49] This IFD protocol complements the essence of our MPS technique by including protein flexibility while docking possible ligands.

The recommended procedures from Schrödinger for IFD were followed. The structural coordinates of MDM2 were obtained from the MDM2−p53 complex (PDB ID: 1YCR[17]). The hydrogens were added, and the protein was prepared according to the recommended protein preparation procedure using the Maestro software package. The active compounds were prepared using LigPrep. Glide XP (extra precision) was used for all docking calculations.[50] The first stage of the IFD protocol performs an initial softened-potential docking of the ligands to the rigid receptor, with van der Waal radii scaling of 0.5 for both MDM2 and the ligands. Sampling of the protein for each of the top 20 ligand poses (ranked by GlideScore) was performed using Prime. Residues within 5 Å of any ligand pose were refined; this consisted of a side-chain conformational search and optimization, followed by full minimization of the residues and the ligand. Complexes within 30.0 kcal/mol of the minimum energy structure were taken forward for redocking. The related ligand was redocked into each low-energy, induced-fit structure with default Glide settings (van der Waal radii scaling of 1.0 for MDM2 and 0.8 for the ligand). Each complex was then ranked according to the IFD score which considers both the docking energy and solvation energy (IFDScore = GlideScore + 5% PrimeEnergy).

Results

Pharmacophore Model. The basic pharmacophore model had six elements: three aromatic/hydrophobic sites and three hydrogen-bond donors. There were also seven excluded volumes which sketch out the rough shape of the binding cleft; the model shown in Figure 1 is detailed further in the Supporting Information. The aromatic/hydrophobic sites agree with the three critical binding residues of p53: Phe19, Trp23, and Leu26. These features also match essential hydrophobic elements of known inhibitors of MDM2. One hydrogen-bond donor element is deep inside the pocket and represents the interaction between the p53 Trp23 indole and the backbone carbonyl of MDM2 Leu54. The other two hydrogen-bond donor elements reflect a consistent interaction with the backbone carbonyls of Gln72 and Val93. These hydrogen bonds are not satisfied by p53, and an increase in binding affinity over the natural substrate could possibly be achieved by taking advantage of these interactions. Although hydrogen bonding to the backbone carbonyls of Gln72 or Val93 has not been exploited by current MDM2−p53 inhibitors, close examination of a cocrystal of MDM2 and a 1,4-benzodiazepine-2,5-dione (PDB ID: 1T4E) may indicate

(46) *MOE*; Chemical Computing Group: Montreal, Canada 2005.
(47) *OMEGA*, version 1.8.b1; OpenEye Scientific Software, Inc.: Santa Fe, NM, 2004.
(48) Nikolovska-Coleska, Z.; Wang, R. X.; Fang, X. L.; Pan, H. G.; Tomita, Y.; Li, P.; Roller, P. P.; Krajewski, K.; Saito, N. G.; Stuckey, J. A.; Wang, S. M. *Anal. Biochem.* **2004**, *332*, 261−273.
(49) Sherman, W.; Day, T.; Jacobson, M. P.; Friesner, R. A.; Farid, R. *J. Med. Chem.* **2006**, *49*, 534−553.
(50) Friesner, R. A.; Murphy, R. B.; Repasky, M. P.; Frye, L. L.; Greenwood, J. R.; Halgren, T. A.; Sanschagrin, P. C.; Mainz, D. T. *J. Med. Chem.* **2006**, *49*, 6177−6196.

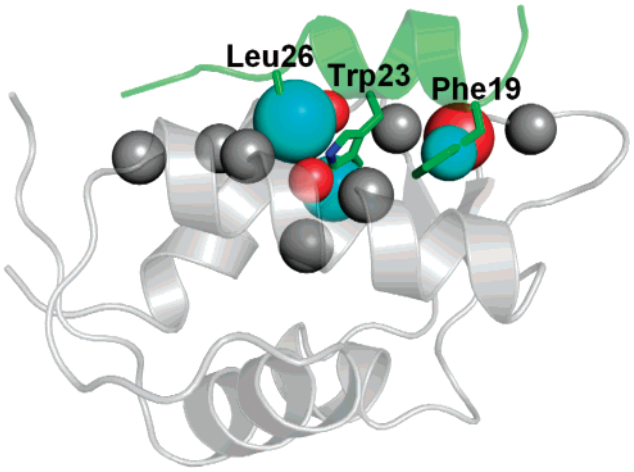

Figure 1. Pharmacophore model for MDM2 with elemental radii based on 2 × rmsd. Cyan is an aromatic/hydrophobic interaction; red is a hydrogen-bond donor, and gray is an excluded volume. MDM2 is shown in gray, and p53 is in green with the side chains of three critical binding residues (Phe19, Trp23, and Leu26) shown in stick representation.

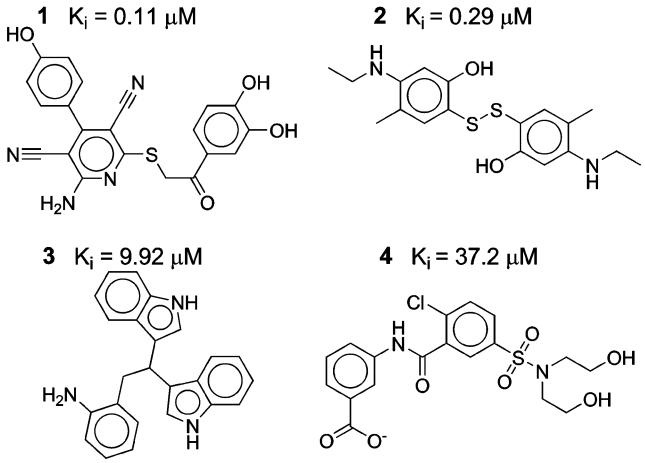

Figure 2. Chemical structures and K_i values of four novel scaffolds which inhibit the MDM2−p53 interaction identified with the MPS method.

such an interaction with the backbone carbonyl of Gln72 is possible. Replacement of the iodo with a cyano group resulted in a large decrease of activity, but the analogous acetylene substituent gave a sub-micromolar compound.[23] This was unexpected considering the size of a cyano group is nearly identical to that of an acetylene group. However, if the terminal hydrogen of the acetylene was polar enough, the orientation of the inhibitor in the binding cleft indicates a dipole−dipole interaction or a weak hydrogen bond could be formed to the backbone carbonyl of Gln72.

Five Novel Scaffolds Are Discovered. Screening the University of Michigan's Center for Chemical Genomics' database of ~35 000 commercially available compounds against the six-site pharmacophore model identified 27 compounds. Of these, 23 were available for purchase (shown in Supporting Information); a fluorescence-polarization-based (FP-based) competitive binding assay showed that four of these compounds were active (17%, compounds **1**−**4** in Figure 2; discovery of the fifth inhibitor is described further below). The competitive binding curves are given in Figure 3. Each scaffold is unique and does not share a substructure with known MDM2 inhibitors. Furthermore, none of the active compounds share a common scaffold with the inactive compounds. The main purpose of the

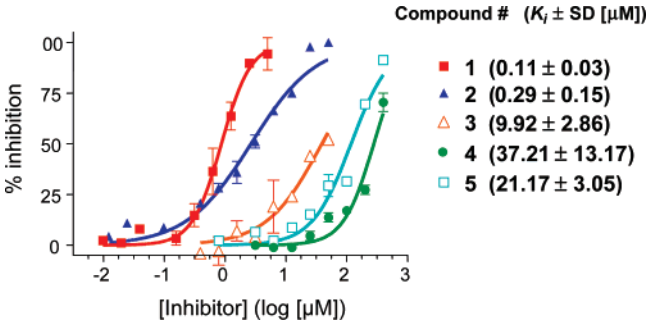

Figure 3. Competitive binding curves of small-molecule inhibitors to MDM2 as determined using a fluorescence-polarization-based binding assay.

MPS method is to push the boundaries of chemical space, to identify leads that are new sizes, shapes, and chemical functionalities. The discovery of four novel inhibitor classes truly demonstrates the applicability of the MPS method in expanding chemical space to identify new inhibitory scaffolds.

Among the four active compounds, **1** has the highest binding affinity with a K_i value of 110 ± 30 nM. To compare this to other known potent inhibitors of the MDM2−p53 interaction, nutlin-3[21] has a K_i value of 36 ± 9 nM in the same competitive binding assay. The peptide which represents the appropriate helix in p53 has a K_i value of 6.67 ± 1.24 μM. Hence, **1** is 3.1 times less potent than nutlin-3, but it is 59 times more potent than the natural substrate. It is important to note that none of the lead molecules have been optimized yet, and there exists a possibility for improving the binding affinity of each compound. However, the discovery with the MPS method of four new scaffolds that inhibit the MDM2−p53 interaction with relatively good potency is highly encouraging. The possibility of identification of further novel scaffolds from screening other, larger datasets against this pharmacophore model should not be dismissed.

Docking the Novel Scaffolds. Docking studies were performed to gain more detailed insight into the structural basis of the binding of our four experimentally verified inhibitors with MDM2. As our method incorporates protein flexibility, it was important that the docking method used accounts for both ligand and receptor flexibility. We chose a novel protein−ligand docking method which combines rigid receptor docking (Glide) with protein structure prediction (Prime) in an induced fit docking (IFD) protocol.[49] It was encouraging to see that the top 14 ranked ligand−protein poses only involved **1**, the most potent compound identified.

Figure 4a shows the binding pose of **1** suggested by the docking protocol. This compound mimics the key hydrophobic residues of p53 when bound to MDM2; the dicyano-substituted pyridinyl moiety projects deep into the Trp23 subpocket. From this pose, it appears that the hydrogen bond to Leu54 is unable to be satisfied due to the orientation of the ring. Although this hydrogen bond is present in all peptide inhibitors and the recently reported spiro-oxindole nanomolar inhibitor,[29,30] many other potent small molecule inhibitors of the MDM2−p53 interaction do not have this feature.[21,23] The catechol moiety occupies the Phe19 subpocket and forms a hydrogen bond with the protein, between one hydroxyl group and the Gln72 backbone carbonyl. The phenol group occupies the Leu26 subpocket. This moiety allows an additional hydrogen bond to be formed, not to Val93 as hypothesized but to the His96 backbone carbonyl.

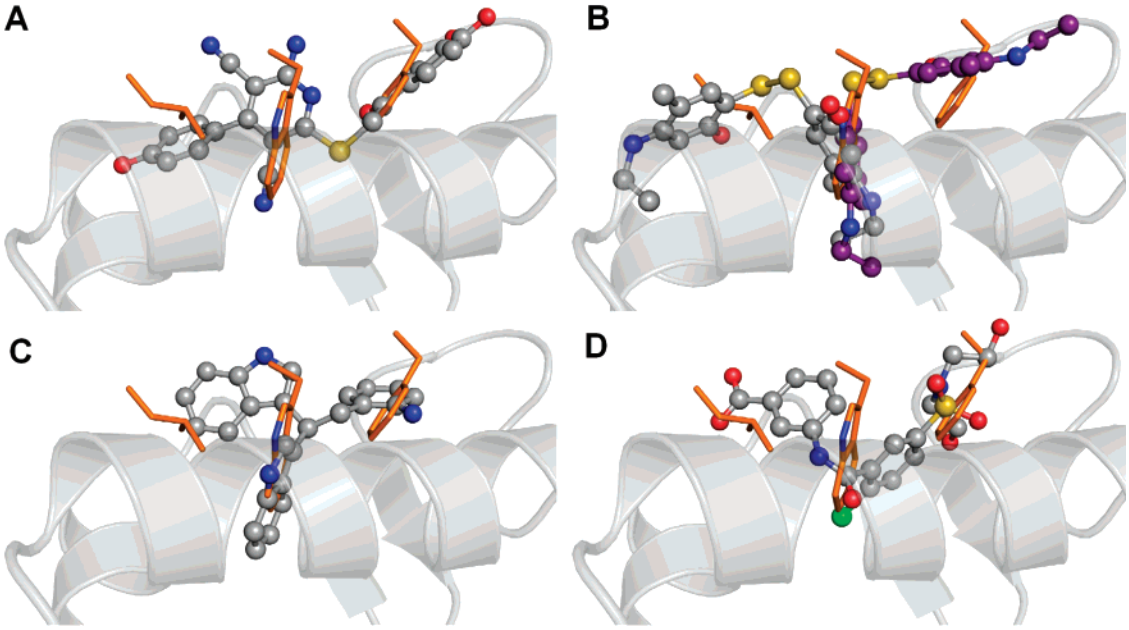

Figure 4. Predicted binding modes of (a) **1**, (b) **2** (two poses), (c) **3**, and (b) **4** to MDM2. Poses were obtained with an induced-fit docking routine from Schrödinger; they are shown in ball and stick representation. MDM2 is shown in gray, with the side chains of Phe19, Trp23, and Leu26 of p53 shown in orange. There are hydrogen bonds present from **1** to the Gln72 and His96 backbone carbonyls, from **2** to the Leu54 backbone carbonyl and either the His96 side-chain NH or Gln72 backbone carbonyl depending on the pose. **3** forms a hydrogen bond to the Leu54 backbone carbonyl, and there are hydrogen bonds from **4** to the Gln72 backbone and side-chain carbonyls.

It is interesting to note that **1** takes a V shape in the cleft, making more hydrophobic contacts with MDM2 than the nutlin or 1,4-benzodiazepine-2,5-dione inhibitors. This shape represents a departure from the "three prong" motif of peptide inhibitors, nutlin and 1,4-benzodiazepine-2,5-dione, emphasizing the ability of the MPS method to identify new shapes of lead molecules.

Comparison to the cocrystal structure of 1,4-benzodiazepine-2,5-dione with MDM2[25] shows that **1** fills the Phe19 subpocket more fully than the iodo group which occupies this space in the cocrystal. The catechol moiety of **1** also mimics the aromatic side chain of Phe19 more accurately than the halogen.[25] One of the cyano substituents, in the Trp23 subpocket, occupies a very similar space to that of the benzo- and chlorophenyl groups of the nutlin[21] and 1,4-benzodiazepine-2,5-dione[25] inhibitors observed in cocrystals with MDM2. This superposition can be seen in the Supporting Information.

Figure 4b shows two possible poses for **2**. In one orientation, the compound occupies the Leu26 and Trp23 sub-pockets and makes hydrogen bonds with the His96 side-chain NH and Leu54 backbone carbonyl. The second pose shows **2** occupying the Trp23 and Phe19 sub-pockets, in this orientation hydrogen bonds are formed with the backbone carbonyls of Leu54 and Gln72.

Although **3** had a more modest K_i value of 9.92 ± 2.86 μM, it was ranked highest after **1** using the IFD protocol. Compound **3** is very hydrophobic, and there were some solubility issues with this compound during the FP-based assay testing which can be seen in the incomplete competitive binding curve (Figure 3). However, we were attracted to the simplicity of the scaffold and its similarity to the key tryptophan of p53. We believe that optimization of the compound could easily improve both the binding affinity and solubility. The binding pose of **3**, shown in Figure 4c, shows one indole moiety mimicking the Trp23 side chain and forming a hydrogen bond to the Leu54 backbone carbonyl, as expected. The positioning of the indole is completely equivalent to that of Trp23 in the cocrystal structure of MDM2−p53.[17] The aminophenyl occupies the Phe19 subpocket while the other indole partially fills the Leu26 subpocket. Clearly, additional substitution off this indole could further complement the Leu26 subpocket and increase the binding affinity of **3** to MDM2.

Figure 4d illustrates the binding mode of **4**, the chloro and carbonyl fill the Trp23 subpocket in a similar manner to that of the nutlin and 1,4-benzodiazepine-2,5-dione. The Leu26 subpocket is occupied by the carboxyphenyl. The two hydroxyethyl groups fill the Phe19 subpocket, where one forms a hydrogen bond to Gln72 O and the other forms one to Gln72 Oϵ1. Again, **4** assumes a V shape in the cleft, to make its contact with the surface, rather than the "three prong" shape assumed by the peptides and other small-molecule inhibitors.

Probing the Hydrophobic Core. Previous analysis of MD simulations and crystal structures of MDM2 had revealed a small hydrophobic pocket deep inside the core of the protein.[32] Probing a possible new binding mode was facilitated by placing an additional seventh hydrophobic pharmacophore element in this pocket (Figure 5a). In this model, the three aromatic/hydrophobic elements, the central donor element (corresponding to Trp23 of p53), and the new hydrophobic element were all required in addition to one of the two remaining donors. Screening of the database yielded 11 hits, 5 of which were available for testing (shown in Supporting Information). Testing with an FP-based competitive binding assay showed compound **5** (20%) had modest activity (K_i = 21.2 μM ± 3.05). Again, this inhibitor does not share a common scaffold with any of the inactive compounds.

To investigate the binding pose of **5**, docking studies with the IFD protocol were again performed. Figure 5b shows **5** mimics two of the critical p53 binding residues (Phe19 and Trp23). The modest K_i value of **5** may be a result of the absence

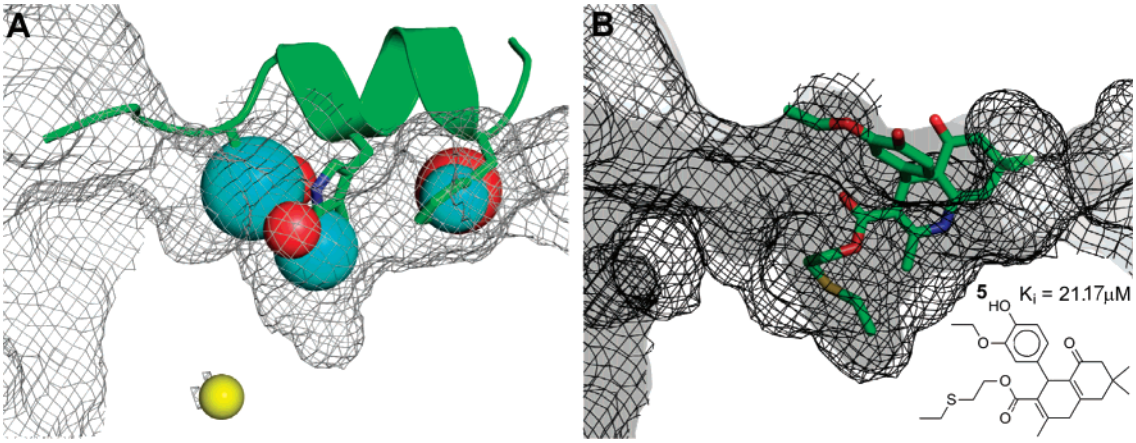

Figure 5. (a) Pharmacophore model for MDM2 with an additional element in the interior hydrophobic core pocket. Elements are shown with a radii multiplication factor of 2: Cyan is an aromatic/hydrophobic interaction; yellow is a hydrophobic interaction, and red is a hydrogen bond donor. The molecular surface of MDM2 is shown as mesh; the p53 peptide is shown in green with the side chains of three key binding residues (Phe19, Trp23, and Leu26) shown in stick representation. (b) The predicted binding mode of **5** is shown. Solid gray shows the starting surface of the pocket (compare to a), and the black mesh shows how the pocket surface has deepened due to the reorganization of the hydrophilic residues. The hydrophobic tail of **5** pushes against the core of MDM2.

of an aromatic moiety in the Leu26 subpocket. In this pose, the ligand does not hydrogen bond to MDM2 and the 3-ethoxy-4-hydroxy phenyl is not bound in the cleft. Reorganization of the Ile103 side chain to occupy the internal hydrophobic pocket allows the Trp23 subpocket to expand. Comparison of the docking structure to cocrystals shows that the hydrophobic tail pushes ~2.5 Å further into the core of MDM2 than p53 and other inhibitors.[17,21,25] Though it does not predict that **5** penetrates into the interior pocket, the IFD protocol comprehensively demonstrates the flexibility in the bottom of the cleft. It seems reasonable that inhibitors may be able to take advantage of the "soft" nature of the bottom of the pocket and its ability to reorganize its contact surface.

Conclusions

The ability of the MPS method in distinguishing known inhibitors from druglike noninhibitors has been well documented.[38−41] However, this work extends verification of the technique to a blind study, where five novel scaffolds for inhibiting the p53−MDM2 interaction were identified from a modest database of commercially available compounds. In addition to the success with chemical diversity, the hit rate was nearly 18% overall. This demonstrates the ability of the MPS method to broadly and efficiently search chemical space to identify a set of diverse inhibitors.

The most potent inhibitor identified, **1**, possessed a K_i value of 110 nM, and this scaffold has yet to be optimized to reach it maximal binding affinity. It may be likely that the binding affinity and specificity could be focused to give highly selective compounds with K_i values in the subnanomolar range. Docking with an induced-fit docking protocol indicted that several of the inhibitors exhibit hydrogen bonds to MDM2 (Gln72, His96, and Leu54 backbone carbonyls and His96 and Gln72 side chains) in addition to the traditional hydrophobic interactions.

The identification of these five novel scaffolds of nonpeptide, small molecule inhibitors to target the MDM2−p53 interaction is an exciting progression for the MPS method. The findings of this work demonstrate that the MPS technique can be used to expand chemical space to discover new inhibitors of protein−protein interactions. It is our hope that further development of this work may lead to a promising new anticancer lead.

Acknowledgment. This work has been supported by the National Institutes of Health (Grant GM65372) and the Beckman Young Investigator Program. For their generous donation of software, we thank Schrödinger for their docking, protein, ligand, and viewing software; OpenEye for OMEGA; and CCG for MOE. We also thank Allen Bailey for maintaining the computers used in this work.

Supporting Information Available: Complete refs 22, 25, 26, 27, and 28; the rmsd analysis of the 21 conformations of MDM2; the coordinates and rmsd of the pharmacophore elements for all models; the 23 inactive compounds tested (based on the six-site pharmacophore model); the 4 inactive compounds tested (based on probing the hydrophobic core of MDM2); and overlays of predicted binding modes of compounds **1**−**4** with crystal structures of nutlin and 1,4-benzodiazepine-2,5-dione. This material is available free of charge via the Internet at http://pubs.acs.org.

JA073687X